Toward an Understanding of the Furoxan−Dinitrosoethylene Equilibrium

John Stevens,† Marcus Schweizer, and Guntram Rauhut*

Contribution from the Institut für Theoretische Chemie, Universität Stuttgart, Pfaffenwaldring 55, 70569 Stuttgart, Germany

Received March 26, 2001

Abstract: The tautomerism of furoxan (1,2,5-oxadiazole-2-oxide) has been investigated by different computational methods comprising modern density functionals as well as single-reference and multi-reference ab initio methods. The ring-opening process to 1,2-dinitrosoethylene is the most critical step of the reaction and cannot be treated reliably by low-level computations. The existence of *cis*−*cis*−*trans*-1,2-dinitrosoethylene as a stable intermediate is advocated by perturbational methods, but high-level coupled-cluster calculations identify this as an artifact. In contrast to the analogous reaction in benzofuroxans, *cis*−*cis*−*cis*-1,2-dinitrosoethylene was found to be a transition state rather than a local minimum. Model potentials were used to explain the occurrence and the disappearing of transition states and local minima relative to the reaction of benzofuroxan. Low-lying triplet states that can be accessed due to spin−orbit coupling were investigated as taking part in alternative routes to a proposed singlet pathway. Barriers for rotations of the nitroso groups on the S_0 and T_1 surfaces are reported.

1. Introduction

The biological importance of compounds containing the N═O group is of increasing interest. Nitric oxide plays an important role as a biological messenger, a macrophage cytostatic agent, a neurotransmitter, and a pressure regulator through binding to the heme group of guanylyl cyclase. Therefore, understanding the chemistry of furoxans (oxadiazole-2-oxide) as a potential nitric oxide generator is of particular importance.[1] Lately, an excellent review about furoxan chemistry has been published.[2]

While experimental[3] and computational studies[4−6] on benzofuroxans are manifold, single-ring furoxans have been studied less extensively.[7−12] However, for both series systematic computational studies on the possible intermediates involved in the tautomeric reaction have been performed.[4,13] Based on photolysis experiments on benzofuroxans and the aforementioned computational studies, it is now widely acknowledged that a 1,2-dinitroso moiety represents the reactive intermediate. Therefore, the reaction can be written as shown in Figure 1. For furoxans, Politzer and co-workers[13−16] used MP4(SDQ) calculations convincingly to rule out the existence of any other intermediates. For 1,2-dinitrosobenzene three conformers can be postulated, while for 1,2-dinitrosoethylene six conformers are in principle allowed. For convenience, we abbreviated the nomenclature of the dinitrosoethylene conformers by using acronyms. Thus, *cis*−*trans*−*cis*-dinitrosoethylene is written in the following as *ctc*-DNE and all other conformers analogously. The structures of all six conformers are displayed in Figure 2. While Politzer and co-workers mainly focused on possible intermediates and their structures, it is the purpose of this study to investigate the complete reaction path including all transition states. One particular aspect concerns *ttt*-DNE. In agreement with Politzer's study, this is the most stable conformer. However, this conformer is not necessarily involved in a thermally induced molecular rearrangement of furoxan. Of course, this may not hold true for photochemically induced reactions, which have been performed in the benzofuroxan series by Murata and Tomioka[17] and other groups.[18,19] Therefore, the question arises whether alternative reaction paths involving intersystem crossings via spin−orbit coupling are of importance which connect the *ttt* conformer to the furoxan rearrangement.

2. Computational Details

Unless otherwise noted, geometries were optimized at the B3-LYP/6-311++G(d,p) level. This gradient-corrected hybrid functional is well known for the proper reproduction of molecular geometries and

* To whom correspondence should be addressed. E-mail: rauhut@theochem.uni-stuttgart.de.

† Deceased, December 2000.

(1) Hwang, K.-J.; Shin, Y. A.; Jo, I.; Yoo, S.; Lee, J. H. *Tetrahedron Lett.* **1995**, *36*, 3337.

(2) Sheremetev, A. B.; Makhova, N. N.; Friedrichsen, W. *Adv. Heterocycl. Chem.* **2001**, *78*, 66.

(3) Vichard, D.; Halle, J.-C.; Huguet, B.; Pouet, M. J.; Riou, D.; Terrier, F. *Chem. Commun.* **1998**, 791.

(4) Ponder, M.; Fowler, J. E.; Schaefer, H. F. *J. Org. Chem.* **1994**, *59*, 6431.

(5) Friedrichsen, W. *J. Phys. Chem.* **1994**, *98*, 12933.

(6) Rauhut, G. *J. Comput. Chem.* **1996**, *17*, 1848.

(7) Paton, R. M. 1,2,5-Oxadiazoles. In *Comprehensive Heterocyclic Chemistry II*; Katritzky, A. R., Rees, C. W., Scriven, E. F. V., Eds.; Pergamon Press: New York, 1996; Vol. 4, p 229.

(8) Śliwa, W.; Thomas, A. *Heterocycles* **1985**, *23*, 399.

(9) Gasco A.; Boulton, A. J. *Adv. Heterocycl. Chem.* **1981**, *29*, 251.

(10) Všetečka, V.; Fruttero, R.; Gasco, A.; Exner, O. *J. Mol. Struct.* **1994**, *324*, 277.

(11) Pasinszki, T.; Westwood, N. P. C. *J. Phys. Chem.* **1995**, *99*, 6401.

(12) Pasinszki, T.; Westwood, N. P. C. *J. Phys. Chem. A* **1998**, *102*, 4939.

(13) Seminario, J. M.; Concha, M. C.; Politzer, P. *J. Comput. Chem.* **1992**, *13*, 177.

(14) Sedano, E.; Sarasola, C.; Ugalde, J. M.; Irazabalbeitia, I. X.; Guerrero, A. G. *J. Phys. Chem.* **1988**, *92*, 5094.

(15) Klenke, B.; Friedrichsen, W. *Tetrahedron* **1996**, *52*, 743.

(16) Godovikova, T. I.; Golova, S. P.; Vozchikova, S. A.; Ignatyeva, E. L.; Povorin, M. V.; Pivina, T. S.; Kmelnizkiy, L. I. *Chim. Geterocycl. Soed.* **1999**, 203.

(17) Murata, S.; Tomioka, H. *Chem. Lett.* **1992**, 57.

(18) Hacker, N. P. *J. Org. Chem.* **1991**, *56*, 5216.

(19) Dunkin, I. R.; Lynch, M. A.; Boulton, A. J.; Henderson, N. *J. Chem. Soc., Chem. Commun.* **1991**, 1178.

10.1021/ja010792c CCC: $20.00
Published on Web 07/07/2001

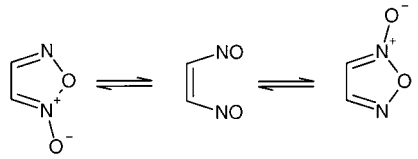

Figure 1. Furoxan−1,2-dinitrosoethylene equilibrium.

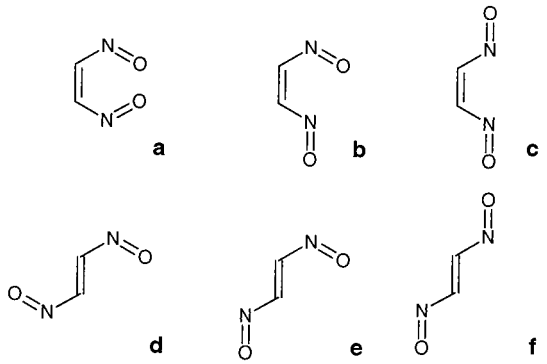

Figure 2. Conformers of 1,2-dinitrosoethylene (a, *ccc*-DNE; b, *cct*-DNE; c, *tct*-DNE; d, *ctc*-DNE; e, *ctt*-DNE; f, *ttt*-DNE).

vibrational frequencies.[20] A comparison with experimental data for furoxan supports these findings. Therefore, zero-point vibrational energies and thermodynamical properties were computed at this level and were eventually transferred to high-level energy single-point calculations. The latter were performed at the coupled-cluster level with a perturbational treatment of the triple excitations, CCSD(T), using a 6-311+G(2df,2pd) basis. In addition, CASPT2 and MRCI calculations based on internally contracted configurations were used to check for multireference effects.[21,22]

Within the multi-reference calculations, two different approaches were used for a proper selection of the active space. First, for the investigation of consecutive structures along a reaction path, an (18,12) active space was chosen, including all π-orbitals, all lone pairs, and the σ-N−O bond to be broken in the ring-opening. The corresponding antibonding orbital was included in the CAS space for each π-orbital and for the σ-bond. Unfortunately, for some structures along the reaction path additional σ-orbitals underwent rotation into the active space during the MCSCF iterations, shifting a corresponding number of lone pairs to the inactive space. This problem was caused by maintaining a consistent active space along the reaction path and by symmetry conditions: it was overcome by freezing all inactive σ-orbitals to the HF orbitals. We believe that this approximation will introduce only a very small error, since the σ-skeleton is not directly involved in the reaction and nevertheless will be correlated in the subsequent perturbational or CI treatment. Second, for calculating different electronic states of the same conformer or the comparison of structures with very different electron distributions, the active space was chosen on the basis of the occupation numbers of the natural orbitals and the magnitude of the CI vectors.[23,24] Consequently, no restrictions were imposed on the type of the orbitals in the active space. Identical active spaces were chosen for the different electronic states of the same conformer. Since the active spaces differ from one conformer to another, small inconsistencies arise in relative energies. However, since relative MRCI and CASPT2 energies are less sensitive with respect to changes in the active space than CASSCF calculations, we consider the resulting differences rather small.

Geometries referring to triplet states were computed at the UB3-LYP level. This was possible since Kohn−Sham methods can be applied without limitations to compute the energy of the lowest triplet state belonging to each irreducible representation of the molecular point group symmetry.[25] Although these geometries are likely to be less reliable than the corresponding singlet structures, electron correlation effects were found to be too important to switch to ROHF wave functions which effectively eliminate spin contamination. As was recently discussed in the literature, the consequences of spin contamination in DFT are not exactly known, but there is strong indication that DFT energies are less affected by spin contamination than UHF results.[26] This is in agreement with the findings of this study: UHF single-point calculations on UB3-LYP optimized structures result in $\langle S^2 \rangle$ expectation values being higher than 2.5 for triplet states, while UB3-LYP values scatter around 2.05 (see below). Although there are several reasons for not using the $\langle S^2 \rangle$ expectation value as a diagnostic for the quality of UDFT energies, it was found that increasing spin contamination also leads to increasing deviation of $\langle S^2 \rangle$ from the exact value.[26] Therefore, we provide $\langle S^2 \rangle$ values for all triplet UB3-LYP calculations. As a consequence of spin contamination, post-HF calculations based on UHF reference wave functions were not taken into account in this study, and hence UB3-LYP relative energies are compared with restricted open-shell coupled-cluster RCCSD(T), CASPT2, and MRCI energies. MRCI energies were corrected for size consistency following Pople's approach (MRCI+P).[27] DFT calculations were performed using GAUSSIAN98,[28] while all other calculations were done with the MOLPRO package of ab initio programs.[29]

3. Comparison with Experimental Data

B3-LYP geometric parameters for furoxan and a comparison with experimental data[30] are provided in Table 1. The agreement with the X-ray results of Godovikova et al. is very good. As was shown recently,[31] the hybrid B3-LYP functional and fourth-order Møller−Plesset perturbation theory are at present the only methods that yield quantitatively correct bond lengths and angles for this species. Since DFT calculations are considerably less demanding than MP4(SDQ) calculations, this investigation relies mainly on B3-LYP geometries. It is the endocyclic N−O bond that is extremely sensitive to electron correlation. The same holds true for benzofuroxans.[32] Therefore, calculations based on MP2 or HF geometries are inherently in error, which may lead to questionable energies. Structures of 1,2-dinitrosoethylene conformers, for which of course no experimental values are available, appear to be less sensitive to correlation effects and are provided by Seminario et al.[13] at the MP2 level.

A further comparison has been performed with respect to the UV spectrum of furoxan. Godovika et al.[30] report an absorption maximum at $\lambda_{max} = 263$ nm in CH_2Cl_2. Equation-of-motion

(20) Rauhut, G.; Pulay, P. *J. Phys. Chem.* **1995**, *99*, 3093.
(21) Werner, H.-J.; Knowles, P. J. *J. Chem. Phys.* **1988**, *89*, 5803.
(22) Celani, P.; Werner, H.-J. *J. Chem. Phys.* **2000**, *112*, 5546.
(23) Pulay, P.; Hamilton, T. *J. Chem. Phys.* **1988**, *88*, 4926.
(24) Bofill, J. M.; Pulay, P. *J. Chem. Phys.* **1989**, *90* 3637.
(25) Gunnarsson, O.; Lundqvist, B. I. *Phys. Rev. B* **1976**, *13*, 4274.
(26) Gräfenstein, J.; Hjerpe, A. M.; Kraka, E.; Cremer, D. *J. Phys. Chem. A* **2000**, *104*, 1748.
(27) Pople, J. A.; Binkley, J. S.; Seeger, R. *Int. J. Quantum Chem. Symp.* **1976**, *10*, 1.
(28) Frisch, M. J.; Trucks, G. W.; Schlegel, H. B.; Scuseria, G. E.; Robb, M. A.; Cheeseman, J. R.; Zakrzewski, V. G.; Montgomery, J. A.; Stratmann, R. E.; Burant, J. C.; Dapprich, S.; Millam, J. M.; Daniels, A. D.; Kudin, K. N.; Strain, M. C.; Farkas, O.; Tomasi, J.; Barone, V.; Cossi, M.; Cammi, R.; Menucci, B.; Pomelli, C.; Adamo, C.; Clifford, S.; Ochterski, J.; Petersson, G. A.; Ayala, P. Y.; Cui, Q.; Morokuma, K.; Malick, D. K.; Rabuck, A. D.; Raghavachari, K.; Foresman, J. B.; Cioslowski, J.; Ortiz, J. V.; Stefanov, B. B.; Liu, G.; Liashenko, A.; Piskorz, P.; Komaromi, I.; Gomperts, R.; Martin, R. L.; Fox, D. J.; Keith, T.; Al-Laham, M. A.; Peng, C. Y.; Nanayakkara, A.; Gonzalez, C.; Challacombe, M.; Gill, P. M. W.; Johnson, B. G.; Chen, W.; Wong, M. W.; Andres, J. L.; Head-Gordon, M.; Replogle, E. S.; Pople, J. A. *Gaussian 98*, Revision A.1; Gaussian, Inc.: Pittsburgh PA, 1998.
(29) MOLPRO is a package of ab initio programs written by H.-J. Werner and P. J. Knowles, with contributions from R. D. Amos, A. Berning, D. L. Cooper, M. J. O. Deegan, A. J. Dobbyn, F. Eckert, C. Hampel, T. Leininger, R. Lindh, A. W. Lloyd, W. Meyer, M. E. Mura, A. Nicklass, P. Palmieri, K. Peterson, R. Pitzer, P. Pulay, G. Rauhut, M. Schütz, H. Stoll, A. J. Stone, and T. Thorsteinsson, Version 99.6, University of Birmingham, UK, 1999 (see http://www.tc.bham.ac.uk/molpro/).
(30) Godovikova, T. I.; Golova, S. P.; Strelenko, Y. A.; Antipin, M. Y.; Struchkov, Y. T.; Khmel'nitskii, L. I. *Mendeleev Commun.* **1994**, 7.
(31) Rauhut, G.; Eckert, F. *Sci. Prog.* **1999**, *82*, 209.
(32) Eckert, F.; Rauhut, G. *J. Am. Chem. Soc.* **1998**, *120*, 13478.

Table 1. Observed and Computed Geometrical Parameters for Furoxan[a]

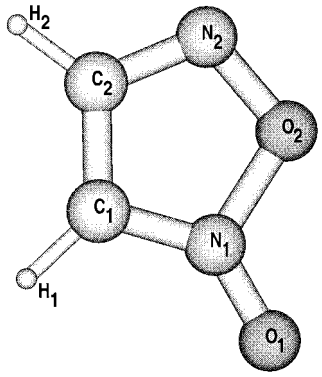

parameter	B3-LYP	expt	parameter	B3-LYP	expt
$r(N_1-O_2)$	1.471	1.441	$\angle(C_1-N_1-O_2)$	105.5	107.2
$r(N_1-C_1)$	1.327	1.302	$\angle(C_2-C_1-N_1)$	107.4	107.2
$r(C_1-C_2)$	1.412	1.401	$\angle(C_1-C_2-N_2)$	111.7	111.9
$r(N_2-C_2)$	1.305	1.292	$\angle(C_2-N_2-O_2)$	107.2	106.6
$r(N_2-O_2)$	1.359	1.379	$\angle(N_1-O_2-N_2)$	108.1	107.1
$r(N_1-O_1)$	1.212	1.240	$\angle(O_1-N_1-O_2)$	118.5	116.4
$r(C_1-H_1)$	1.075	(0.92)	$\angle(O_1-N_1-C_1)$	136.0	136.4
$r(C_2-H_2)$	1.079	(0.97)	$\angle(H_1-C_1-N_1)$	120.3	(123)
			$\angle(H_2-C_2-N_2)$	120.3	(120)

[a] Bond lengths in angstroms and bond angles in degrees. Geometrical parameters in parentheses denote the uncertainties associated with the determination of hydrogen positions from X-ray data.

coupled-cluster calculations without the inclusion of triple excitations, EOM-CCSD, yield a maximum at 243 nm for a $\pi-\pi^*$ ($X \rightarrow 1^1A'$) excitation. Although EOM-CCSD is well known for its systematic overestimation of excitation energies due to an unbalanced description of the ground and excited states, the discrepancy observed in this case still must be considered large.[33] For this reason we have also performed an EOM-CCSD calculation based on a state-averaged MCSCF wave function. This approach leads to a small correction and yields an absorption maximum at 247 nm. The results indicate that triples corrections are desirable. In addition, we have performed time-dependent B3-LYP calculations and obtained an excitation at 254 nm, which is in resonable agreement with the experimental value. With an oscillator strength two magnitudes lower than the excitation under consideration, there is a nearby A'' state at 259 nm (TD-B3-LYP).

4, Relative Stabilities

Initially, the energies of all DNE conformers relative to furoxan were studied; the results are summarized in Table 2. In agreement with the experimental findings, all DNE conformers are considerably higher in energy than furoxan. However, the computed relative stabilities of all conformers with respect to furoxan vary significantly, depending on the level of theory. For instance, the perturbational triples correction in the coupled-cluster approach (i.e., CCSD vs CCSD(T)) shifts the DNE conformers to higher energies by approximately 5 kcal/mol. We ascribe this to an inproper description of the electronic wave function of the reference molecule (i.e., furoxan) rather than as originating from the DNE conformers. This is corroborated by the T_1 diagnostic of Taylor and Lee.[34,35] The T_1 value of furoxan (0.020) is higher than the corresponding values for all DNE conformers (0.017), indicating that the triples correction has more impact on furoxan than on the dinitrosoethylenes. Due to this sensitivity, the CCSD(T) level is mandatory for a proper ab initio treatment of these systems. However, the DFT energies are closer to the CCSD(T) results than the CCSD energies and thus provide a good starting guess at a fraction of the computational effort.

Table 2. Relative Energies (kcal/mol) of Furoxan and All Conformers of 1,2-Dinitrosoethylene[a]

structure	symmetry	B3-LYP	CCSD	CCSD(T)	ZPE
furoxan	C_s	0.0	0.0	0.0	30.9
cct-DNE	C_1	33.3	24.6	29.5	
ctc-DNE	C_i	35.4	25.7	30.5	28.4
ctt-DNE	C_1	30.0	21.6	26.7	28.5
tct-DNE	C_{2v}	30.3	21.3	26.5	28.5
ttt-DNE	C_{2h}	26.6	18.1	23.4	28.7

[a] All energies refer to a 6-311+G(2df,2pd) basis set and do not include any corrections due to the zero-point vibrational energy (ZPE) etc. ZPEs were computed at the DFT level. Except for *cct*-DNE, all structures were optimized at the B3-LYP/6-311++G** level. The structure of *cct*-DNE was determined at the MP4(SDQ)/6-311+G** level.

The most stable DNE conformer found by all methods is *ttt*-DNE, while *ctc*-DNE is the highest in energy. The first result is in agreement with the MP4(SDQ)/6-31G* results of Politzer and co-workers[13] but in contrast to the HF/6-31G** results of Sedano et al.,[14] the latter also being in contradiction to the HF/6-31G* results of Politzer's study. However, Politzer et al. found *ccc*-DNE to be highest in energy, while our results here indicate that this is a transition state (see below) and consequently *ctc*-DNE is the highest local minimum. Despite the repulsion between the nitrogen lone pairs, *tct*-DNE was found to have C_{2v} symmetry. Most likely, conjugation of the N=O π-orbitals with the C=C double bond overcompensates this repulsive orbital interaction. *ctc*-DNE shows C_i symmetry, while a C_{2h} structure refers to a transition state connecting the two possible enantiomeric C_i conformers. The barrier was found to be below 3.5 kcal/mol at the B3-LYP level (without ZPE correction). The same situation was observed for *ctt*-DNE: a planar C_s structure is a transition state between two enantiomeric C_1 conformers. The activation barrier (without ZPE correction) is 0.9 kcal/mol. Consequently, the exact symmetry of this conformer does not have any impact on the reaction mechanism. Most interestingly, all conformers with a nitroso group in cis orientation avoid planarity, although one would expect better π-conjugation for these structures.

Of particular interest is the structure of *cct*-DNE. Politzer and co-workers found a local minimum for this structure at the HF/6-31G* and MP2/6-31G* levels, which was confirmed by frequency calculations. In contrast to this, we did not find a stationary point at the B3-LYP level. However, geometry optimizations at the MP4(SDQ)/6-311+G** level again converged to the *cct*-structure found by Politzer's group. Relative energies of this structure as provided in Table 2 refer to the MP4(SDQ) geometry. At this stage it was not possible to reach a final conclusion regarding the existence of *cct*-DNE. However, as will be discussed in the next section, a detailed investigation of the ring-opening process indicates that an energy minimum for *cct*-DNE cannot be found at the CCSD(T) or CASPT2-(18,12) levels. Therefore, we believe that the local minimum found by HF or MP*n* methods are artifacts of the methods arising from neglecting all or at least static electron correlation effects. B3-LYP, however, includes dynamical correlation in

(33) Hampe, O.; Koretsky, G. M.; Gegenheimer, M.; Huber, C.; Gauss, J. *J. Chem. Phys.* **1997**, *107*, 7085.

(34) Lee, T. J.; Taylor, P. R. *Int. J. Quantum Chem.* **1989**, *23*, 199.

(35) Taylor, P. R. In *Accurate Calculations and Calibration*; Roos, B. O., Ed.; Lecture Notes in Chemistry 58; Springer-Verlag: Heidelberg, 1992; p 325.

Table 3. Vertical $S_0 \rightarrow T_1$ Energies (kcal/mol) for *ttt*-DNE

method	ΔE
(U)B3-LYP	15.1
CASPT2	−0.5
CASPT3	54.0
MRCI+P	26.2
(R)CCSD	46.7
(R)CCSD(T)	27.6

the correlation functional and recovers contributions to the static electron correlation in the exchange functional.[36,37] In the case of *o*-dinitrosobenzenes, the corresponding structure to *cct*-DNE indeed is a local minimum but is also sensitive to the correlation level.[32]

Nitroso compounds are well known for their low-lying triplet states. Moreover, rotations of NO groups around the C=C double bond often involve triplet states or open-shell singlets. The latter are of importance for the photoinduced cis−trans isomerization of stilbene but play no role in the thermally induced ring−chain tautomerism of furoxan. To test the reliability of the computational methods for the triplet states in detail, the vertical $S_0 \rightarrow T_1$ gap of the highly symmetrical (and thus computationally efficient) *ttt* conformer was computed by a variety of methods. The results are summarized in Table 3. As indicated by the large difference between the CASPT2 and CASPT3 gaps, the perturbational CAS methods appear to be of limited use for the systems investigated here. Only the most sophisticated methods, i.e., CCSD(T) and MRCI+P, agree in their prediction and are thus the only methods that can safely be interpreted. For these reasons we have computed relative energies of the triplet states at the UB3-LYP, the restricted open-shell coupled-cluster, RCCSD(T), and the MRCI+P levels. Two sets of reference structures were chosen: first, the relaxed B3-LYP structures of the singlet states and second, the relaxed UB3-LYP structures of the lowest biradicaloid triplet states. Results are provided in Table 4. With the exceptions of *tct*- and *ctt*-DNE, for each conformer the same molecular point group was found for the stationary points on the S_0 and T_1 surfaces. However, the two electronically excited states of each conformer may belong to different irreducible representations (e.g. *ttt*-DNE). While T_1 *ctt*-DNE shows C_s symmetry, this corresponds to a transition state on the ground-state surface (see above). The RCCSD(T) and MRCI+P singlet−triplet gaps (either vertical or adiabatic) agree nicely for all DNE conformers investigated. Since the MRCI+P calculations were computationally feasible only for symmetric structures and due to the excellent agreement between the RCCSD(T) and MRCI+P results, even for the adiabatic gaps, we restricted all further calculations to the RCCSD(T) and UB3-LYP levels. The UB3-LYP calculations provide energy gaps which are consistently lower by approximately −10 kcal/mol than at the ab initio levels. This indicates that UB3-LYP calculations lead to an exaggerated stabilization of the triplet states. Due to the small adiabatic $S_0 \rightarrow T_1$ gaps, this culminates in the prediction of triplet ground states for *ctt*-, *tct*-, and *ttt*-DNE, which is not supported by the RCCSD(T) and MRCI+P calculations. To judge whether this is a general failure of the B3-LYP functional or holds true only for the systems studied here, further systematic computational studies are highly desirable.

Considering the vertical $S_0 \rightarrow T_1$ gap of *ctc*-DNE, the ^3A_g state was found to be only 1.7 (MRCI+P) or 2.7 kcal/mol (RCCSD(T)), respectively, lower in energy than a corresponding ^3A_u state. This order is reversed at lower correlation levels. Notably, no closed-ring furoxan structure can be found on the UB3-LYP triplet surface. Instead, a planar open-ring structure was computed that resembles the singlet *cct*-DNE conformer. Consequently, the triplet open-ring furoxan (or planar triplet *cct*-DNE, respectively) is much closer in energy to the triplet DNE conformers than the S_0 furoxan to the DNE conformers on the closed-shell surface. The T_1 open-ring furoxan is essentially identical in energy (without ZPE correction) with triplet *ccc*-DNE, which in contrast to the S_0 structure was found to be a true local minimum rather than a transition state.

5. The Furoxan Ring-Opening

The furoxan ring-opening toward *cct*-DNE, and subsequently to *tct*-DNE, along a singlet reaction path critically depends on the level of computation. Politzer and co-workers[13] found that *instead of a single, clearly defined transition state, the MP2/6-31G* potential curve reaches a plateau, extending over a range of N−O distances of at least 0.86 Å and characterized by a number of points each satisfying the criterion for a transition state*. A relaxed B3-LYP potential energy scan for rotation about the C−N bond, shown in Figure 3, confirms the findings of Politzer et al. The structure at a CCNO dihedral of 0° represents furoxan, at about 100° the transition state, and at 180° *tct*-DNE. As mentioned above, the *cct* conformer was not found at the B3-LYP level, but at the MP4(SDQ) level, showing a dihedral of 53°. In this region the B3-LYP potential indeed is very shallow but shows no ditch as found by Politzer and our MP4(SDQ) studies. Therefore, the stationary point at about 98° primarily represents the saddle point, corresponding to the rotation of the nitroso group between the (nonexistent) *cct*-DNE and *tct*-DNE rather than being the transition state of the ring-opening. The latter was found at the MP4(SDQ) level at 17°. This cannot be explained by the B3-LYP potential shown in Figure 3. However, it can easily be explained by a much steeper potential at low dihedrals, indicating that at the MP4(SDQ) level the reaction is determined by an in-plane N−O stretching at the beginning and a subsequent out-of-plane rotation of the nitroso group as the reaction proceeds. In case of the B3-LYP potential, both processes are strongly coupled, and the increase of the potential is much softer at the beginning but shifts the transition state of the bond cleavage toward the *cct* conformer. The strong overlap of the potentials of the internal in-plane and the out-of-plane coordinates essentially causes the local minimum corresponding to *cct*-DNE to vanish (vide infra).

To judge whether the B3-LYP or the MP4(SDQ) results are correct, we performed CCSD(T) and CASPT2 calculations on all B3-LYP and MP4(SDQ) structures along this reaction path. Results are provided in Table 5. Note that the CASPT2 results shown in Table 5 are expected to be of higher quality than the CASPT2 results for the $S_0 \rightarrow T_1$ gap discussed above, since the computational problems at this level of theory arise solely from the description of the triplet state. The B3-LYP, CCSD(T), and CASPT2 results consistently indicate that the structure of *cct*-DNE obtained by an MP4(SDQ) geometry optimization is higher in energy than the transition state between furoxan and *cct*-DNE. Consequently, *cct*-DNE cannot be found at these levels, and therefore we conclude that a local minimum on the potential surface does not exist for *cct*-DNE. However, the CCSD energies support the MP4(SDQ) results, demonstrating again the importance of the triples contribution as long as the structural motif of furoxan is involved in energetic considerations. In comparison to the CCSD(T) results, all CASPT2 energies are

(36) Baerends, E. J.; Gritsenko, O. V. *J. Phys. Chem.* **1997**, *101*, 5383.
(37) Gritsenko, O. V.; Schipper, P. R. T.; Baerends, E. J. *J. Chem. Phys.* **1997**, *107*, 5007.

Table 4. Vertical and Adiabatic $S_0 \rightarrow T_1$ Energies (kcal/mol) for Furoxan and All Dinitrosoethylene Conformers[a]

	vertical						adiabatic						
structure	symmetry	T_1	$\langle S^2\rangle_{KS}$	DFT[b]	CC[c]	MRCI[d]	symmetry	T_1	$\langle S^2\rangle_{KS}$	DFT[b]	CC[c]	MRCI[d]	ZPE
furoxan	C_s	$^3A'$	2.02	64.8	71.6	72.3	C_s	$^3A'$	2.02	20.9	31.7	34.2	29.0
cct-DNE	C_1	^3A	2.12	12.5	23.0		*e*	*e*	*e*	*e*	*e*	*e*	*e*
ctc-DNE	C_i	^3A_g	2.04	16.6	26.8	25.5	C_i	^3A_g	2.00	0.7	14.1	14.3	31.0
ctt-DNE	C_1	^3A	2.04	14.0	21.9		C_s	$^3A''$	2.07	−2.5	10.6		28.9
tct-DNE	C_{2v}	$^3B_1$	2.04	11.6	25.1	24.4	C_2	$^3A''$	2.07	−0.9	18.2[f]		29.8
ttt-DNE	C_{2h}	^3B_g	2.03	15.1	27.6	26.2	C_{2h}	^3B_u	2.01	−7.7	7.3	7.7	28.7

[a] All energies refer to a 6-311+G(2df,2pd) basis set and do not include any corrections due to the zero-point vibrational energy etc. ZPEs were computed at the DFT level. Except for *cct*-DNE, all structures were optimized at the B3-LYP/6-311++G** level. The structure of *cct*-DNE was determined at the MP4(SDQ)/6-311+G** level. [b] B3-LYP and UB3-LYP calculations. [c] CCSD(T) and RCCSD(T) calculations. [d] MRCI+P results. [e] There is no triplet structure corresponding to the singlet *cct* conformer at the UB3-LYP level (see text). [f] While UB3-LYP calculations predict the $^3A''$ state to be lowest in energy, the RCCSD(T) energy gap refers to a $^3A'$ state.

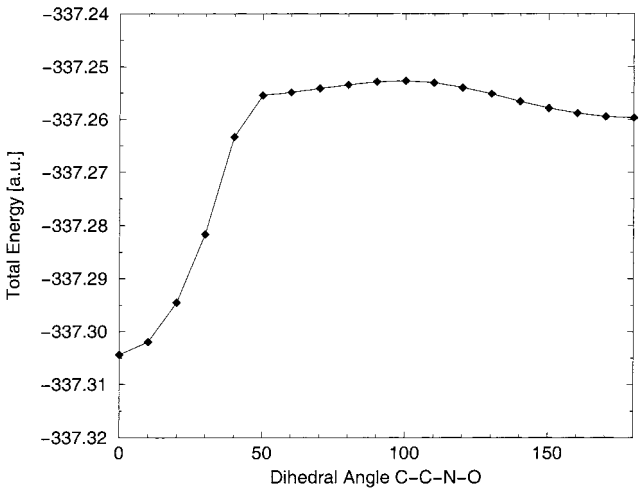

Figure 3. Energy profile of the ring-opening process along the CCNO dihedral.

Table 5. Relative Energies (kcal/mol) of All Stationary Points along the Singlet Reaction Path of the Ring-Opening Process of Furoxan[a]

structure	B3-LYP	CCSD	CCSD(T)	CASPT2	ZPE
furoxan	0.0	0.0	0.0	0.0	30.9
TS(furoxan → *cct*-DNE)	24.8	31.0	27.5	36.3	
cct-DNE	33.9	24.6	29.5	36.6	
TS(*cct*-DNE → *tct*-DNE)	34.7	25.6	31.2	38.3	28.0
tct-DNE	30.3	21.3	26.5	32.6	28.5

[a] All energies refer to a 6-311+G(2df,2pd) basis set and do not include any corrections due to the zero-point vibrational energy (ZPE) etc. ZPEs were computed at the DFT level. Except for *cct*-DNE and TS(furoxan → *cct*-DNE), all structures were optimized at the B3-LYP/6-311++G** level. The structures of *cct*-DNE and TS(furoxan → *cct*-DNE) were determined at the MP4(SDQ)/6-311+G** level.

increased by at least 6 kcal/mol. We ascribe this to the generally observed finding[38,39] that CASPT2 is not fully converged with respect to dynamical correlation, which is of particular importance for furoxans and benzofuroxans. Note that, in the case of benzofuroxan and *o*-dinitrosobenzene, single-reference MP2 also significantly underestimates the relative stability of the dinitrosobenzene conformers and the corresponding transition states.[31,32] Therefore, we consider the CCSD(T) barrier of 31.2 kcal/mol the most reliable value. This value is lowered by the zero-point vibrational energy (ZPE) to 28.3 kcal/mol (without scaling of the ZPE).

In analogy to the rearrangement in benzofuroxans, one needs to consider the possibility of a singlet reaction from furoxan via the nonexistent *cct*-DNE toward *ccc*-DNE. However, despite being very similar in structure to the corresponding intermediate *ccc*-dinitrosobenzene (*ccc*-DNB), *ccc*-DNE is a transition state rather than a local minimum (Figure 4). To understand this result, we used empirically determined model potentials as depicted in Figure 5. The plot on the left (1) represents the situation in benzofuroxan: the potential for the in-plane ring-opening (A) overlaps with the rotation of one nitroso group (B). The primed energy profiles denote the identical potentials for the in-plane ring closure (A′) and the rotation of the other nitroso group (B′). The additive A+B and A′+B′ potentials (dotted lines) and the most relevant total energy profile (bold line), which represents the reaction profile along the intrinsic reaction coordinate, are also shown. Note that, after the ring-opening, the A potentials converge toward a discrete value rather than zero since the corresponding planar dinitroso compound is higher in energy than the furoxan. As found for benzofuroxans, the overall reaction is dominated by the ring-opening process followed by a series of local minima (*cct*-DNB and *tct*- or *ccc*-DNB, respectively) and transition states characterized by the rotational barriers. The second plot, (2), describes the situation for the rearrangement of furoxan via *tct*-DNE. Slight modifications of the potentials, mainly affecting the one for the ring-opening (A), alter the situation—with respect to (1)—completely: the minima corresponding to *cct*-DNE vanish and the point highest in energy essentially corresponds to the rotation of the nitroso group as discussed above. The main modification applied is a higher resulting potential of A once the barrier for the ring-opening has been passed. The argument for this modification is evident: in the case of benzofuroxan, the open-ring product (i.e., any *o*-dinitrosobenzene) is stabilized by strong conjugation effects which transform the quinoide six-membered ring into an aromatic benzene ring. Of course, this effect does not affect the potential of the unsubstituted furoxan, and consequently, the resulting potential is shifted to higher values. As a result, the overall reaction barrier is much higher for the rearrangement of furoxan than for benzofuroxan (compare models (1) and (2)), as indeed is found by the ab initio calculations. Moreover, as found by Politzer et al. and as shown

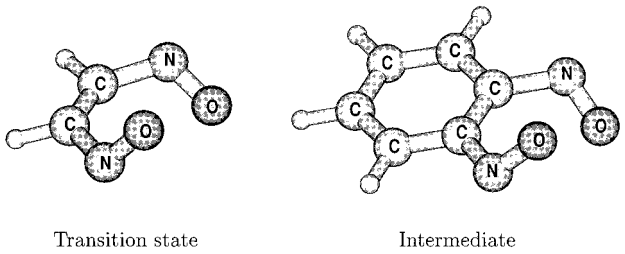

Figure 4. Structures of *cis*−*cis*−*cis*-dinitrosoethylene and *syn*-dinitrosobenzene.

(38) Werner, H.-J. *Mol. Phys.* **1996**, *89*, 645.
(39) Christiansen, O.; Gauss, J.; Stanton, J. F.; Jorgensen, P. *J. Chem. Phys.* **1999**, *111*, 525.

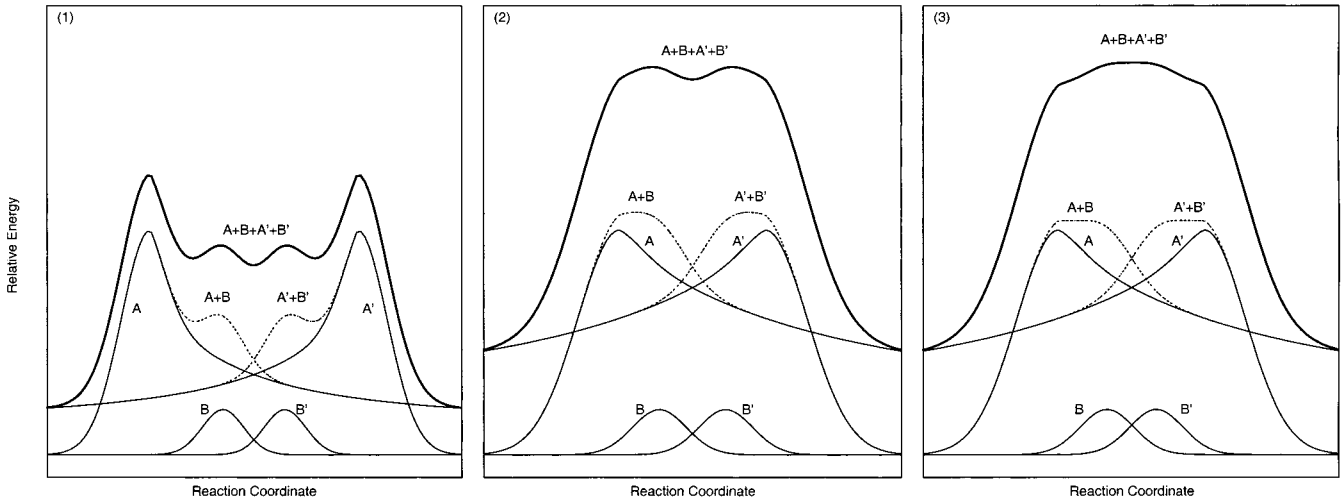

Figure 5. Model potentials explaining the different reactions of the ring-opening in furoxans and benzofuroxans.

in Figure 3, the region of the transition state is characterized by a plateau. The last model (plot (3), right) describes the situation of the rearrangement of furoxan via *ccc*-DNE. The A potentials remain the same as in the last model, since the ring-opening process does not change. However, the rotations of the nitroso groups are much more strongly coupled in this case, which is simulated by a larger overlap of the B potentials. As a consequence, the minimum in the overall potential vanishes and *ccc*-DNE appears as a transition state. Once more, the region of the transition state is very flat, and the barrier observed is higher than for the other two model situations. All effects discussed are in agreement with the findings for the reactions of furoxan, and thus the *ccc*-moiety represents a local minimum in one case and a transition state in the other.

The assumptions of the model can be proven by a simple study. As proposed above, the fused transition state corresponding to *ccc*-DNE originates from the coupling of the two nitroso groups in cis orientation. Consequently, a decoupling of the nitroso groups, which in terms of the model potentials results in shifting the B potentials apart, should change the character of *ccc*-DNE (i.e., intermediate vs transition state). This can be achieved by constraint geometry optimizations of *ccc*-DNE. Freezing the C═C distance to predefined values and optimizing all other geometrical parameters should alter the nature of *ccc*-DNE, as can be checked by frequency calculations. In Figure 6, the lowest eigenvalue of the force constant matrixes are plotted against the (fixed) C═C distance. For transition states this eigenvalue must be negative (imaginary frequency), while a local minimum has only positive eigenvalues. At a C═C distance of about $r = 1.37$ Å, the character of *ccc*-DNE changes. Consequently, *ccc*-DNE with a C═C distance of 1.345 Å appears as a transition state, while *syn*-dinitrosobenzene (i.e., *ccc*-DNB) with a C═C distance of 1.414 Å is a minimum. This example shows that the nature of the *ccc* moiety and thus the height of the corresponding reaction barrier can be controlled by appropriate substituents at the carbon atoms. Similiar arguments can be applied to the plateaulike transition state of the ring-opening via *tct*-DNE.

As an alternative to these singlet reaction paths, we also focused on a triplet path including intersystem crossings. This path is characterized by a rotation about the central C═C bond from furoxan to *ctt*-DNE and has been investigated by a relaxed potential energy scan of the NCCN dihedral. Starting from the triplet structure of furoxan, the scan has been performed for a triplet wave function obtained at the UB3-LYP level and is

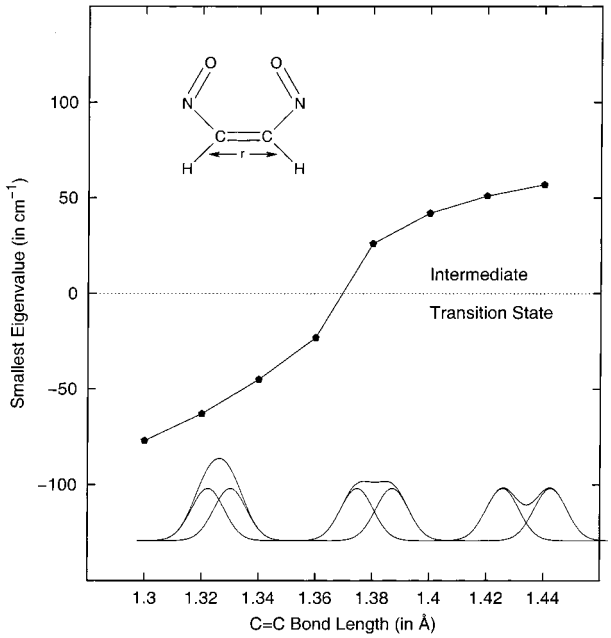

Figure 6. Lowest eigenvalue of the force constant matrix of *cis*−*cis*−*cis*-dinitrosoethylene, dependent of the C═C distance *r*.

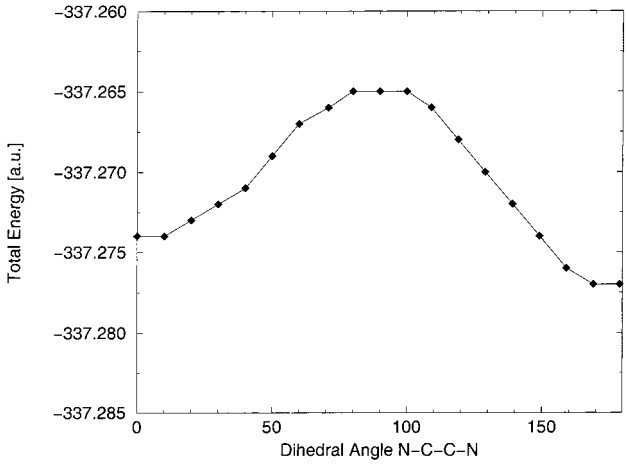

Figure 7. Triplet energy profile of the rotation about the C═C double bond along the NCCN dihedral.

shown in Figure 7. The triplet transition state of this reaction path is only 26.6 kcal/mol (without ZPE correction) higher in

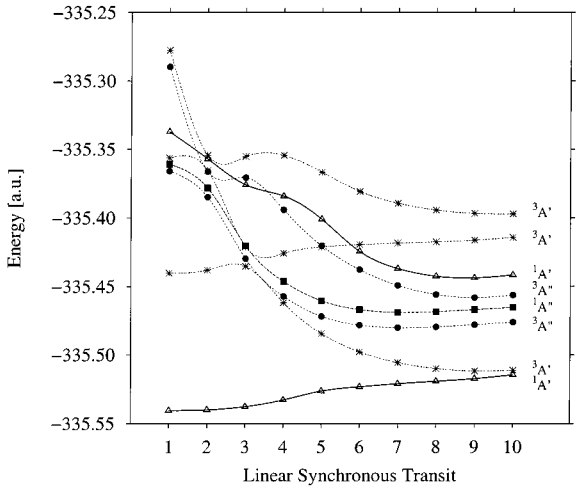

Figure 8. Triplet and singlet energy profile along a linear synchronous transit from the singlet to the triplet furoxan structure.

energy than the S_0 furoxan ground state at the UB3-LYP/6-311+G(2df,2pd) level and is thus 8.1 kcal/mol below the transition state of the singlet pathway. By contrast, relative to the S_0 transition state, the T_1 transition state is 5.1 kcal/mol higher in energy at the RCCSD(T) level. Relative to the RCCSD(T) value, UB3-LYP calculations predict the T_1 transition state to be −13.0 kcal/mol lower in energy. This stabilization is exactly in the same range as discussed above for the $S_0 \rightarrow T_1$ gaps, for which the RCCSD(T) results were found to be in excellent agreement with multireference CISD results. Therefore, we consider the lower transition state on the T_1 surface an artifact of the B3-LYP density functional rather than mirroring the physical situation. However, since the difference between the two transition states at the RCCSD(T) level is not too large, triplet stabilizing substituents at the central C═C bond may alter the situation.

For this reason we have investigated this alternative reaction in more detail by computing a linear synchronous transit (LST) starting from the (closed-ring) singlet structure of furoxan toward the corresponding (open-ring) triplet structure. For the singlet−triplet gap of the latter structure, significant differences can be found depending on the method. While UB3-LYP predicts the triplet state to be significantly stabilized relative to the singlet state, the gap shrinks to 0.8 kcal/mol at the RCCSD(T) level. CASPT2 even reverses the order and predicts S_0 to be still more stable than T_1 by −2.6 kcal/mol. A state-averaged CASSCF-(14,11) calculation of the LST is shown in Figure 8. Structure 1 refers to the furoxan S_0 minimum, and structure 10 corresponds to the open-ring T_1 minimum. The adiabatic representation of the states shown in this diagram shows several avoided crossings affecting the triplet state under investigation. The lowest $^3A'$ state and the singlet reference state come extremely close as the LST proceeds. Therefore, a spontaneous intersystem crossing would, in principle, allow the alternative reaction path to compete with the singlet pathway. Nonadiabatic coupling between these two states can arise only as a result of spin−orbit interaction. We have calculated the spin−orbit matrix element between $^1A'$ and $^3A'$ on CASSCF level using the full Breit−Pauli Hamiltonian, the only nonvanishing element being over the z component ($M_S = 0$) due to symmetry conditions. The transition probability between these two states including spin−orbit corrections is proportional to the square of the transition dipole moment, the latter being a function of the spin−orbit matrix element. The transition dipole moment is thus $|\mu| = 1.2 \times 10^{-5}$ D. This value is large enough to allow for an $X^1A' \rightarrow 1^3A'$ transition. Consequently, the further course of the reaction is determined by the energetic difference between the singlet and triplet transition states (i.e., furoxan (S_0) to *tct*-DNE (S_0) vs furoxan (T_1) to *ctt*-DNE (T_1)). As dicussed above, in the case under consideration the difference is too large to allow for a side reaction via the triplet surface.

Table 6. Transition-State Energies (kcal/mol) of Singlet and Triplet Structures Connecting the Different Conformers of 1,2-Dinitrosoethylene (Relative to Furoxan)

structure	state	DFT[a]	CC[b]	ZPE[c]
TS(*ctt*-DNE → *ctc*-DNE)	S_0	36.3	33.3	27.7
TS(*tct*-DNE → *ttt*-DNE)	S_0	34.7	39.5	27.2
TS(*ctt*-DNE → *ttt*-DNE)	S_0	32.8	29.6	27.9
TS(*ctt*-DNE → *ctc*-DNE)	T_1	32.2	43.6	28.2
TS(*tct*-DNE → *ttt*-DNE)	T_1	33.2	36.6	28.3
TS(*ccc*-DNE → *ctc*-DNE)	T_1	26.8	36.2	28.9
TS(*ctt*-DNE → *ttt*-DNE)	T_1	30.8	43.1	27.9
TS(*cct*-DNE → *ccc*-DNE)	T_1	32.7	44.1	28.2
TS(*cct*-DNE → *tct*-DNE)	T_1	33.2	45.1	28.0
TS(*cct*-DNE → *ctt*-DNE)	T_1	26.6	36.3	28.6

[a] B3-LYP or UB3-LYP results, respectively. [b] CCSD(T) or RCCSD(T) results, respectively. [c] ZPEs were computed at the DFT level.

6. Rotational Barriers

The furoxan ring-opening has been augmented by studying the links between the different conformers of 1,2-dinitrosoethylene. Since reactions on the S_0 and the T_1 surfaces appear to be possible, most barriers have been computed for both states. Table 6 summarizes the energies of the transition states relative to singlet furoxan. Assuming that simultaneous rotations of both nitroso groups are without relevance for the reaction mechanism, and considering the finding that the singlet hypersurface allows only for four DNE conformers, there remain just three transitions states to be trapped on the S_0 surface. The most remarkable results concern the transition state between *tct*-DNE and *ttt*-DNE: at the CCSD(T) level it is only 8.3 kcal/mol (without ZPE correction) higher in energy than the transition state of the furoxan ring-opening. Its C_2 structure is characterized by a C−C single bond of 1.47 Å and a symmetrical charge distribution. The corresponding transition state on the T_1 surface is just 2.9 kcal/mol lower at the RCCSD(T) level.

As must be expected, rotations of the nitroso groups about the C−N bonds (for instance, *ctc*-DNE to *ctt*-DNE) exclusively prefer the S_0 surface, whereas rotations about the central C═C double bond are likely to involve the low-lying T_1 state. In other words, for rotations about the central C═C bond, the T_1 transition states are lower than the corresponding S_0 barriers. The triplet transition states of the N−O rotations are remarkable in the sense that the N−O group actually does not literally rotate, but the oxygen atom moves via a linear C−N−O moiety at the transition state toward the product conformation. As an example, the T_1 transition state between *tct*-DNE and the open-ring T_1 furoxan (or *cct*-DNE, respectively) is shown in Figure 9.

The last three transition states listed in Table 6 characterize the reactions that connect the T_1 furoxan (or T_1 *cct*-DNE, respectively) to the other DNE conformers. All these barriers are above the S_0 transition states that link S_0 furoxan to the DNE hypersurface. As mentioned above, besides these barriers that are relevant for the mechanism under investigation, other transition states were trapped that link some DNE conformers with their mirror images which are identical in energy. This concerns the *ctt* and *ctc* conformers.

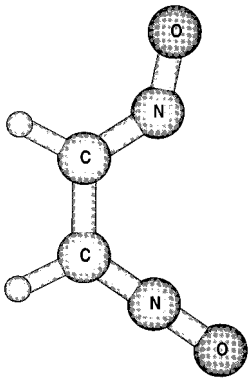

Figure 9. Structure of the transition state between *trans−cis−trans*-1,2-dinitrosoethylene and furoxan on the triplet T_1 surface.

7. Conclusions

The ring−chain tautomerism of furoxan via 1,2-dinitrosoethylene has been investigated in detail, and in total 26 stationary points were found. The rearrangement of unsubstituted furoxan is determined by a singlet pathway which is slightly lower in energy than an alternative reaction involving a low-lying triplet state that can be reached through spin−orbit coupling. The relative energy difference between a relaxed open-ring triplet structure of furoxan and the parent S_0 compound is too large and hence makes low-lying triplet states irrelevant for the studied species. Since the preferred reaction mechanism involves only *tct*-DNE as an intermediate, *ctc*-, *ctt*-, and *ttt*-DNE are likely not to be involved in the thermally induced reaction. *cct*-DNE could not be identified as a stable intermediate as in the case of benzofuroxans. *ccc*-DNE was found to be a transition state that describes a one-step rearrangement of furoxan. The corresponding barrier of this step lies between the lowest transition state of the reaction and the barrier via the triplet surface. Since the lowest computed reaction barrier of 28.3 kcal/mol (including ZPE corrections) is rather high, substituents are of significant importance for observing this rearrangement under standard conditions. However, the nature of a substituent introduced may also have a significant impact on the underlying mechanism, as could be shown on the basis of model potentials. These potentials indicate that the ring−chain tautomerism of furoxan is characterized by fused transition states, i.e., those which originate from a superposition of the potentials of at least two fundamental transition states. The occurrence and disappearance of these fused transition states and thus the height of the overall reaction barrier can be controlled by the substituents connected to the carbon atoms. Hence, the entire reaction can easily be controlled by the electronic nature of the substituents in the 3- and 4-positions of oxadiazole-2-oxides.

From a computational viewpoint, in comparison to CCSD(T) energies, the B3-LYP functional gives reasonable estimates of relative energies on the S_0 surface. However, open-shell triplet structures are predicted to be too stable at the UB3-LYP level (in comparison to RCCSD(T) and MRCI calculations), which must be considered unreliable for the systems investigated in this study. As found in related studies, dynamical electron correlation effects are very important for this class of molecules, which even limit the use of the CCSD and CASPT2 approaches.

Acknowledgment. We thank Prof. A. R. Katritzky and Dr. S. Denisenko for valuable discussions and Prof. N. N. Makhova for providing us with a copy of the UV spectrum of furoxan. Computer time at the Institut für Theoretische Chemie, Stuttgart, is kindly acknowledged.

Supporting Information Available: Tables of Cartesian Coordinates (PDF). This material is available free of charge via the Internet at http://pubs.acs.org.

JA010792C